GEOPHYSICAL RESEARCH LETTERS, VOL. 36, L01306, doi:10.1029/2008GL036364, 2009

Predicting the geodetic signature of $M_W \geq 8$ slow slip events

Brendan J. Meade[1] and John P. Loveless[1]

Received 17 October 2008; revised 20 November 2008; accepted 1 December 2008; published 7 January 2009.

[1] Elastic dislocation models of geodetic measurements above subduction zones have led to the identification of $M_W \approx 6.0-7.2$ slow slip events (SSEs) that release elastic strain over periods of days to months, but great ($M_W \geq 8$) SSEs have remained unidentified. We extrapolate observations of SSE duration and slip magnitude to show that slip velocity decreases with event magnitude and predict that the slip velocity of $M_W \geq 8$ SSEs is $\leq$50 mm/yr. The slip velocity for great SSEs may never exceed the plate convergence rate and thus never produce a reversal in trench perpendicular motion. Instead, geodetically constrained estimates of apparent partial elastic coupling on subduction zone interfaces worldwide may be direct observations of ongoing $M_W \geq 8$ silent earthquakes with durations of decades to centuries. **Citation:** Meade, B. J., and J. P. Loveless (2009), Predicting the geodetic signature of $M_W \geq 8$ slow slip events, *Geophys. Res. Lett.*, *36*, L01306, doi:10.1029/2008GL036364.

1. Introduction

[2] Fault slip that occurs with a period of days or longer and fails to generate damaging seismic waves defines the occurrence of a silent earthquake or slow slip event (SSE). While the first such event was recognized along the central San Andreas fault [*Linde et al.*, 1996], current catalogs show that most SSEs occur in active subduction zones [*Ide et al.*, 2007; *Schwartz and Rokosky*, 2007]. These events have been identified by time-dependent geodetic observations of crustal deformation in the overriding plate above subduction zones including Cascadia [*Dragert et al.*, 2001; *Miller et al.*, 2002], New Zealand [*Douglas et al.*, 2005; *Wallace and Beavan*, 2006], Nankai [*Hirose et al.*, 1999; *Obara et al.*, 2004], central Japan [*Ozawa et al.*, 2002], and Guerrero [*Kostoglodov et al.*, 2003; *Larson et al.*, 2007]. Throughout the duration of an SSE, thrust sense slip on the subduction zone interface elastically deforms the overriding plate, generating coseismic sense surface displacements toward the trench [*Dragert et al.*, 2001]. These displacements are opposite to the sense of motion that characterizes the locked behavior of a fault during the nominal interseismic period [*Savage*, 1983] and is thus termed a reversal. Geodetic reversals are often considered the diagnostic signature of SSEs and have been used to constrain temporal and spatial characteristics of SSE slip. Here we use event duration and slip magnitude estimates to show that average SSE slip velocity, v_{SSE}, decreases with event magnitude and is well described by a law derived from ordinary earthquake (OE) magnitude-area relationships [*Wells and Coppersmith*, 1994], creep event stress drop estimates [*Brodsky and Mori*, 2007], and the SSE magnitude-duration relationship [*Ide et al.*, 2007]. If $M_W \geq 8$ SSEs exist, slip velocities are predicted to generally be less than plate convergence rates at subduction zones, v_s (<120 mm/yr). In fact, the predicted slip velocity of great SSEs is slow enough (<50 mm/yr) and their durations long enough (>10 years) that $M_W \geq 8$ SSEs may never exceed the rate of subduction and thus never produce a geodetic reversal. Instead, thrust sense SSE slip may release a fraction of the accumulating strain, creating the appearance of a partially coupled subduction zone (as inferred from elastic dislocation models of nominally interseismic geodetic measurements; hereinafter referred to as "apparent partial elastic coupling") that is a snapshot in the time evolution of an ongoing $M_W \geq 8$ SSE.

2. A Slip Velocity Law for Slow Slip Events

[3] We define the average velocity of coseismic sense slip during an SSE as the total slip divided by the event duration, $v_{SSE} = s/T$. We consider SSE duration to define the total interval of time over which an event occurs, which may include along strike migration, rather than the period of detection at a single geodetic station. SSE velocities computed from observations of the durations (Figure 1a) and slip magnitudes of previously recognized SSEs [*Schwartz and Rokosky*, 2007] show a decrease in v_{SSE} with magnitude from 2,000–3,000 mm/yr at $M_W = 6$ to 70–400 mm/yr at $M_W \approx 7.2$ (Figure 1b). We derive a slip velocity law consistent with these observations by considering empirical scaling relationships for SSE duration, stress drop, and OE rupture area. *Ide et al.* [2007] found a linear relationship between SSE moment, M_0, and event duration, T, $M_0 \approx T \times 10^{\tau}$ ($\tau = 12-13$), that holds over nine orders of magnitude in moment (Figure 1a). Substituting this definition of T and slip, s, as a function of seismic moment, $s = M_0/\mu A$, into the definition of average velocity gives $v_{SSE} = 10^{\tau}/\mu A$, where μ is the crustal shear modulus. Empirical studies of OE dimensions have shown that rupture area, A (km^2), scales with moment magnitude as $\log_{10} A = a + bM_W$ [*Wells and Coppersmith*, 1994]. We extrapolate this relationship to the sparsely observed $M_W > 8$ regime neglecting any possible break in scaling at large OE magnitude. Estimated scaling values for OEs of all slip styles are $a = -3.49 \pm 0.16$, $b = 0.91 \pm 0.03$, while for the thrust style slip that characterizes subduction zones, $a = -3.99 \pm 0.36$, $b = 0.98 \pm 0.06$ [*Wells and Coppersmith*, 1994]. Estimates of creep event stress drops have revealed that, for a given seismic moment, the area over which a creep event occurs is 10–100 times larger than that of an OE [*Brodsky and Mori*, 2007]. This order of magnitude increase in rupture area can be incorporated into an SSE magnitude-area scaling law by modifying the *Wells and Coppersmith* [1994] OE scaling law coefficient a such

[1]Department of Earth and Planetary Sciences, Harvard University, Cambridge, Massachusetts, USA.

0094-8276/09/2008GL036364$05.00

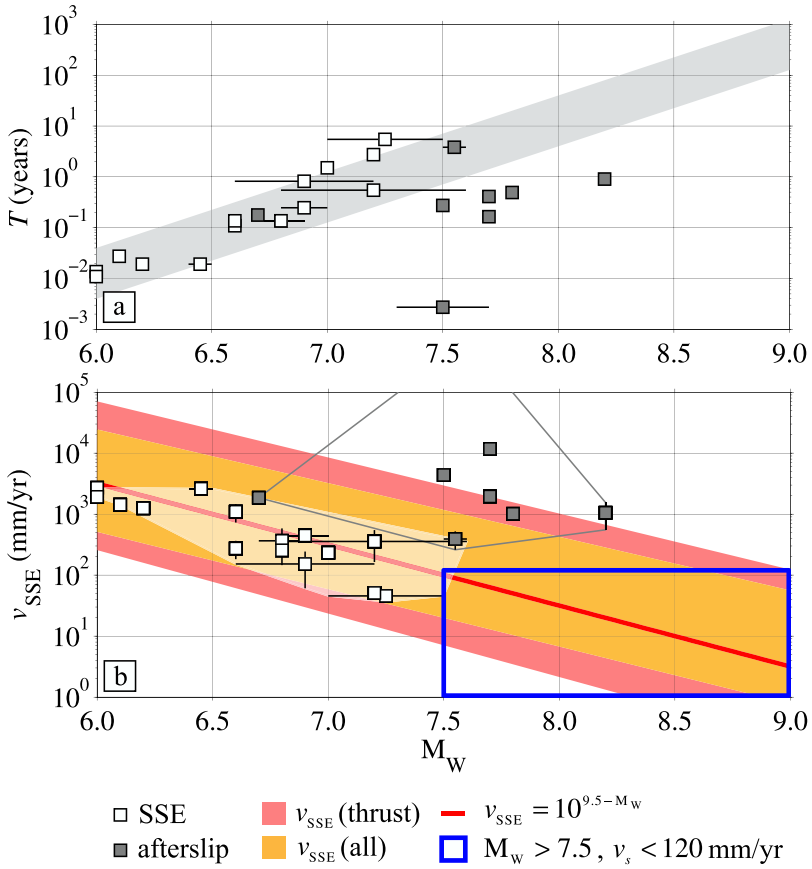

Figure 1. Slow slip event duration and slip velocity as a function of magnitude. SSEs are from the *Schwartz and Rokosky* [2007] compilation where duration, displacement, and scalar moment are reported. White squares are SSEs that occurred in the absence of macroscopic seismic triggering while dark gray squares are SSEs classified as post-seismic. Black lines represent reported uncertainties. (a) Observed SSE duration, *T*, and *Ide et al.* [2007] scaling law (gray shading) shows the increase in event duration with magnitude. (b) Mean slip velocity and derived scaling laws. The regions shaded in white and outlined in gray show the convex hulls encompassing each of the two classes of SSEs. Note that there is negligible overlap between these two slip velocity regimes. Pink and orange shading indicate the minimum and maximum bounds on the slip velocity derived from the thrust and inclusive ordinary earthquake rupture area scaling laws, respectively [*Wells and Coppersmith*, 1994]. An approximate analytic expression, $v_{SSE} = 10^{9.5\text{-}M_W}$ (mm/yr), is shown as a red line. The region outlined in blue highlights SSEs with $M_W > 7.5$ and $v_{SSE} < 120$ mm/yr (less than the convergence rate at most subduction zones), which would not be expressed as reversals in geodetic position time series but rather as apparent partial elastic coupling.

that $a' = a + 1$ (km^2) or $a' = a + 7$ (m^2). With this definition of SSE rupture area, the average SSE slip velocity, v_{SSE} (in m/s), as a function of magnitude is

$$\log_{10} v_{SSE} = \tau - (\log_{10} \mu + a' + bM_W). \quad (1)$$

By combining the estimated scaling values from *Ide et al.* [2007] and *Wells and Coppersmith* [1994], and assuming a characteristic shear modulus of 30 GPa we find $\log_{10} v_{SSE} = (-1.49 \pm 0.66) - (0.91 \pm 0.03)M_W$ averaged over all styles of slip (Figure 1b). Focusing on rupture area scaling for thrust earthquakes [*Wells and Coppersmith*, 1994] characteristic of subduction zones, we find $\log_{10} v_{SSE} = (-0.99 \pm 0.86) - (0.98 \pm 0.06)M_W$ (with the concise approximation $v_{SSE} = 10^{9.5\text{-}M_W}$ mm/yr). The SSE slip velocity law agrees remarkably well with all of the observed events excluding those that represent afterslip following an OE (Figure 1b). The nature of this distinction may result from the generation of large-scale coseismic stresses or an ambiguity in the determination of the dominant post-seismic deformation process. To avoid the possibility of incorrectly combining the effects of two separate phenomena, we focus our analysis on the SSEs that emerge in the absence of triggering by macroscale seismicity.

3. Geodetic Signature of Great Slow Slip Events

[4] Our derived scaling law makes the testable prediction that the average slip velocity for a $M_W \geq 8.0$ SSE should be $\leq$50 mm/yr (Figure 1b). Such a slip velocity may not exceed the rate of plate convergence, $v_s \approx 20$–120 mm/yr, at the subduction zones where SSEs are most likely to occur (Figure 1b). For this case, where $v_{SSE} < v_s$, the combined effects of SSE slip and interseismic strain accumulation will not produce net thrust sense slip on the subduction zone interface during the SSE. Thus, the anticipated geodetic signature of a $M_W \geq 8$ SSE is not a reversal in motion in the

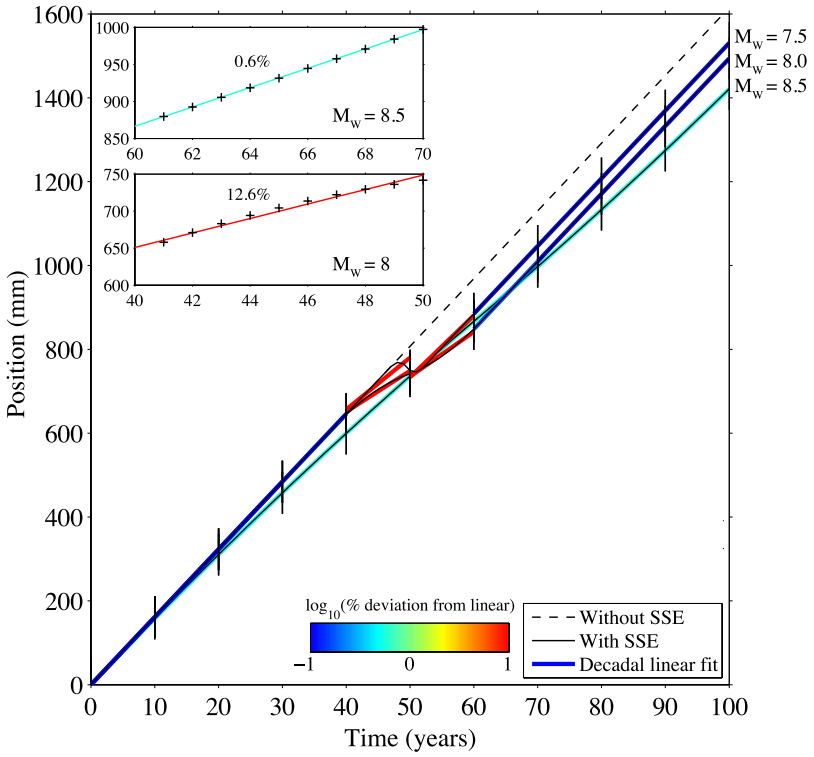

Figure 2. Synthetic position time series at a geodetic monument 100 km away from the trench of a subduction zone dipping at 25°. The three colored lines show the position evolution for M_W = 7.5, 8.0, and 8.5 SSEs with durations of T = 4, 22, and 123 years and mean v_{SSE} of 145, 47, and 15 mm/yr, respectively. A M_W = 9.0 SSE, with duration 694 years and mean v_{SSE} of 5 mm/yr, is indistinguishable from the steady state, fully coupled interseismic signal (black dashed line) over the first 100 years of its duration. The vertical black lines mark decadal intervals characteristic of the longest observation period of continuous geodetic networks. Line color indicates the percent deviation from linearity over any 10-year interval. The ten year intervals with the maximum deviation from linearity (∼0.6% and ∼12.6% for M_W = 8.5 and M_W = 8.0 SSEs, respectively) are shown in the upper and lower inset panels.

overriding plate as has been observed for smaller events [*Dragert et al.*, 2001]. Instead, the net rate of slip deficit between the downgoing slab and the overriding plate at the subduction zone interface will be $v_s - v_{SSE}$, reducing the rate of elastic strain accumulation in the overriding plate. This predicted signature of large SSEs has been previously interpreted as apparent partial elastic coupling on the plate interface using nominally steady state geodetic velocities and elastic dislocation models in the Japan [*Nishimura et al.*, 2004], Nankai [*Gao and Schmidt*, 2006], Cascadia [*Wang et al.*, 2003], Kamchatka [*Bürgmann et al.*, 2005], New Zealand [*Wallace et al.*, 2004], Alaska [*Freymueller and Beavan*, 1999], Sumatra [*Simoes et al.*, 2004], Central America [*Norabuena et al.*, 2004], South America [*Khazaradze and Klotz*, 2003], and Guerrero [*Larson et al.*, 2004] subduction zones. In each of these regions, the fraction of apparent partial elastic coupling, χ, has been mapped between two end member models, complete coupling, $\chi = 1$, and zero coupling (fault creep), $\chi = 0$, while the possibility that net thrust sense motion may be ongoing is generally excluded [*Larson et al.*, 2004; *Wallace et al.*, 2004]. These pervasive observations of apparent partial elastic coupling are exactly the predicted signature of $M_W \geq 8.0$ SSEs and can also be used to infer SSE slip velocities, $v_{SSE} = v_s(1 - \chi)$.

[5] Because a $M_W \geq 8$ SSE would occur over such a long period and continuous geodetic time series rarely span more than 10 years, it is not yet possible to observe more than a snapshot of large SSE time evolution. However, initial observations of time-variable apparent elastic coupling, such as that discovered in northern Honshu [*Nishimura et al.*, 2004] and northern New Zealand [*Árnadóttir et al.*, 1999], may allow for indirect imaging of the time history of evolving SSE slip velocity as the duration of geodetic time series increases. Over a decadal time scale, the rate change in SSE slip velocity may be quite small (<5 mm/yr^2) and may appear approximately linear in geodetic time series (Figure 2). The gradual change in surface measurements of these events can be seen in synthetic geodetic time series for independent M_W = 7.5, 8.0, 8.5, and 9.0 SSEs with periods of T = 4, 22, 123, and 694 years, and v_{SSE} of 145, 47, 15, and 5 mm/yr, respectively. We calculate displacement time series at an observation located 100 km from the trench, above a subduction zone interface dipping 25°, extending to a depth of 40 km, and subject to steady coseismic slip deficit applied at a rate of v_s = 50 mm/yr, characteristic of an intermediate convergence rate subduction zone (e.g., Cascadia or Nankai). Time-dependent thrust sense SSE slip on the deepest 20 km of the fault, assuming a symmetric, constant acceleration, triangular source-time function, is superimposed on the classical fully locked subduction zone model [*Savage*, 1983] to produce a composite displacement time series. The synthetic position time series for the

M_W = 7.5 SSE case shows a ~4-year long reversal in motion where the annual displacement is toward the trench rather than away from the trench as predicted by the steady fully locked case (Figure 2). This behavior is similar to the largest of the previously identified SSEs including the M_W < 7.2, Bungo Channel (Japan) SSE in 1997 [*Gao and Schmidt*, 2006] and the M_W < 7.6 Guerrero SSE in 2001 [*Kostoglodov et al.*, 2003]. In contrast, throughout the longer duration of M_W = 8.0, 8.5, and 9.0 SSEs (T = 22, 123, and 694 years respectively) thrust sense slip never exceeds the subduction rate and the maximum deviation from linearity over any ten year period is ~12.6% for a M_W = 8.0 SSE and ~0.6% for a M_W = 8.5 SSE (Figure 2), suggesting that extended duration geodetic time series will provide additional constraints on the temporal evolution of SSE behavior.

4. Discussion and Conclusions

[6] Geodetic detection of apparent partial elastic coupling may be interpreted in several ways, including 1) steady creep on the plate interface at a rate slower than that of plate convergence, 2) an imaging or modeling artifact, or, as we propose here, 3) the temporary effect of great SSEs. Previously, this signal has been interpreted as an indication of variations in material properties of the subduction zone interface governed by the thickness of subducted sediments, pore fluid pressure, and/or the location of seismic asperities. The dewatering of subducted oceanic slabs [*Kodaira et al.*, 2004], increases in subduction interface temperature [*McCaffrey et al.*, 2008], and inferred changes in frictional conditions [*Liu and Rice*, 2005] below the seismogenic zone are consistent with the location of SSEs. However, the fact that SSEs occur at shallower levels [*Douglas et al.*, 2005; *McCaffrey et al.*, 2008] indicates that simple depth-dependent variables are not sufficient to explain the occurrence of all SSEs. SSEs occurring at depths more typical of seismogenesis (<40 km) also coincide with regions of apparent partial elastic coupling [*McCaffrey et al.*, 2008; *Wallace and Beavan*, 2006]. Further, observed temporal variations in apparent partial elastic coupling [*Árnadóttir et al.*, 1999; *Nishimura et al.*, 2004] could be well explained as a result of time-dependent SSE slip rather than coordinated macroscopic changes in subduction zone properties.

[7] The possible existence of $M_W \geq 8$ SSEs raises critical questions with regard to both the mechanics and evolution of subduction zones as well as seismic hazard along the most active plate boundary zones. Rate and state friction laws can explain the emergence and <1-year duration of $M_W \approx$ 6.0–7.2 SSEs [*Liu and Rice*, 2005] such as those previously documented in the Cascadia, Nankai, and Guerrero subduction zones. Understanding the mechanics behind great SSEs may enable the prediction of the magnitude-frequency distribution and constrain the potential maximum size of these events. The creep event slip-area relationship [*Brodsky and Mori*, 2007] suggests that a M_W = 9.0 SSE would occur over a rupture area ~10^6 km^2, which may be precluded by the extent of contiguous subduction zone interface unless there is a scale-dependent physics that increases SSE stress drop at large magnitudes. Assuming a dip of 20° and elastic strain accumulation between 10 and 40 km depth, the Japan-Kamchatka, Aleutian, Sumatra, and South American subduction zones have contiguous areas of approximately 2.6 × 10^5, 3.3 × 10^5, 4.2 × 10^5, 5.0 × 10^5 km^2 and may theoretically support SSEs with maximum magnitudes of M_W = 8.6, 8.7, 8.8, and 8.9, respectively, if simultaneous activity along these interfaces were defined as representing a single SSE.

[8] Future studies utilizing dense geodetic networks will develop robust maps of both instantaneous and time-dependent apparent partial elastic coupling that will allow for a detailed accounting of the SSE seismic moment released and the development of time-dependent probabilistic seismic hazard assessment. For example, if the frequency and magnitude of great SSEs are independent of the plate convergence rate, then more slowly slipping subduction zones, such as the Caribbean, may release the majority of accumulated elastic strain during SSEs rather than OEs, providing a possible mechanism to explain the apparent dearth of historical seismic moment release [*Stein et al.*, 1982].

[9] **Acknowledgments.** We thank Kelin Wang and an anonymous referee for constructive reviews. This research was supported by funding from Harvard University.

References

Árnadóttir, T., S. Thornley, F. F. Pollitz, and D. J. Darby (1999), Spatial and temporal strain rate variations at the northern Hikurangi margin, New Zealand, *J. Geophys. Res.*, *104*, 4931–4944.

Brodsky, E. E., and J. Mori (2007), Creep events slip less than ordinary earthquakes, *Geophys. Res. Lett.*, *34*, L16309, doi:10.1029/2007GL030917.

Bürgmann, R., M. G. Kogan, G. M. Steblov, G. Hilley, V. E. Levin, and E. Apel (2005), Interseismic coupling and asperity distribution along the Kamchatka subduction zone, *J. Geophys. Res.*, *110*, B07405, doi:10.1029/2005JB003648.

Douglas, A., J. Beavan, L. Wallace, and J. Townend (2005), Slow slip on the northern Hikurangi subduction interface, New Zealand, *Geophys. Res. Lett.*, *32*, L16305, doi:10.1029/2005GL023607.

Dragert, H., et al. (2001), A silent slip event on the deeper Cascadia subduction interface, *Science*, *292*(5521), 1525–1528.

Freymueller, J. T., and J. Beavan (1999), Absence of strain accumulation in the western Shumagin segment of the Alaska subduction zone, *Geophys. Res. Lett.*, *26*(21), 3233–3236.

Gao, H., and D. A. Schmidt (2006), The slip history of the 2004 slow slip event on the northern Cascadia subduction zone, *Eos Trans. AGU*, *87*(52), Fall Meet. Suppl., Abstract T41A-1540.

Hirose, H., K. Hirahara, F. Kimata, N. Fujii, and S. Miyazaki (1999), A slow thrust slip event following the two 1996 Hyuganada earthquakes beneath the Bungo Channel, southwest Japan, *Geophys. Res. Lett.*, *26*(21), 3237–3240.

Ide, S., et al. (2007), A scaling law for slow earthquakes, *Nature*, *447*(7140), 49–50.

Khazaradze, G., and J. Klotz (2003), Short- and long-term effects of GPS measured crustal deformation rates along the south central Andes, *J. Geophys. Res.*, *108*(B6), 2289, doi:10.1029/2002JB001879.

Kodaira, S., T. Iidaka, A. Kato, J.-O. Park, T. Iwasaki, and Y. Kaneda (2004), High pore fluid pressure may cause silent slip in the Nankai Trough, *Science*, *304*(5675), 1295–1298.

Kostoglodov, V., S. K. Singh, J. A. Santiago, S. I. Franco, K. M. Larson, A. R. Lowry, and R. Bilham (2003), A large silent earthquake in the Guerrero seismic gap, Mexico, *Geophys. Res. Lett.*, *30*(15), 1807, doi:10.1029/2003GL017219.

Larson, K. M., A. R. Lowry, V. Kostoglodov, W. Hutton, O. Sánchez, K. Hudnut, and G. Suárez (2004), Crustal deformation measurements in Guerrero, Mexico, *J. Geophys. Res.*, *109*, B04409, doi:10.1029/2003JB002843.

Larson, K. M., V. Kostoglodov, S. Miyazaki, and J. A. S. Santiago (2007), The 2006 aseismic slow slip event in Guerrero, Mexico: New results from GPS, *Geophys. Res. Lett.*, *34*, L13309, doi:10.1029/2007GL029912.

Linde, A. T., M. T. Gladwin, M. J. S. Johnston, R. L. Gwyther, and R. G. Bilham (1996), A slow earthquake sequence on the San Andreas fault, *Nature*, *383*(6595), 65–68.

Liu, Y., and J. R. Rice (2005), Aseismic slip transients emerge spontaneously in three-dimensional rate and state modeling of subduction earthquake sequences, *J. Geophys. Res.*, *110*, B08307, doi:10.1029/2004JB003424.

McCaffrey, R., et al. (2008), Slow slip and frictional transition at low temperature at the Hikurangi subduction zone, *Nat. Geosci.*, *1*(5), 316–320.

Miller, M. M., T. Melbourne, D. J. Johnson, and W. Q. Sumner (2002), Periodic slow earthquakes from the Cascadia subduction zone, *Science*, *295*(5564), 2423–2423.

Nishimura, T., et al. (2004), Temporal change of interplate coupling in northeastern Japan during 1995–2002 estimated from continuous GPS observations, *Geophys. J. Int.*, *157*(2), 901–916.

Norabuena, E., et al. (2004), Geodetic and seismic constraints on some seismogenic zone processes in Costa Rica, *J. Geophys. Res.*, *109*, B11403, doi:10.1029/2003JB002931.

Obara, K., H. Hirose, F. Yamamizu, and K. Kasahara (2004), Episodic slow slip events accompanied by non-volcanic tremors in southwest Japan subduction zone, *Geophys. Res. Lett.*, *31*, L23602, doi:10.1029/2004GL020848.

Ozawa, S., et al. (2002), Detection and monitoring of ongoing aseismic slip in the Tokai region, central Japan, *Science*, *298*(5595), 1009–1012.

Savage, J. C. (1983), A dislocation model of strain accumulation and release at a subduction zone, *J. Geophys. Res.*, *88*, 4984–4996.

Schwartz, S. Y., and J. M. Rokosky (2007), Slow slip events and seismic tremor at circum-Pacific subduction zones, *Rev. Geophys.*, *45*, RG3004, doi:10.1029/2006RG000208.

Simoes, M., J. P. Avouac, R. Cattin, and P. Henry (2004), The Sumatra subduction zone: A case for a locked fault zone extending into the mantle, *J. Geophys. Res.*, *109*, B10402, doi:10.1029/2003JB002958.

Stein, S., J. F. Engeln, D. A. Wiens, K. Fujita, and R. C. Speed (1982), Subduction seismicity and tectonics in the lesser Antilles arc, *J. Geophys. Res.*, *87*, 8642–8664.

Wallace, L. M., and J. Beavan (2006), A large slow slip event on the central Hikurangi subduction interface beneath the Manawatu region, North Island, New Zealand, *Geophys. Res. Lett.*, *33*, L11301, doi:10.1029/2006GL026009.

Wallace, L. M., J. Beavan, R. McCaffrey, and D. Darby (2004), Subduction zone coupling and tectonic block rotations in the North Island, New Zealand, *J. Geophys. Res.*, *109*, B12406, doi:10.1029/2004JB003241.

Wang, K., R. Wells, S. Mazzotti, R. D. Hyndman, and T. Sagiya (2003), A revised dislocation model of interseismic deformation of the Cascadia subduction zone, *J. Geophys. Res.*, *108*(B1), 2026, doi:10.1029/2001JB001227.

Wells, D. L., and K. J. Coppersmith (1994), New empirical relationships among magnitude, rupture length, rupture width, rupture area, and surface displacement, *Bull. Seismol. Soc. Am.*, *84*(4), 974–1002.

J. P. Loveless and B. J. Meade, Department of Earth and Planetary Sciences, Harvard University, 20 Oxford Street, Cambridge, MA 02138, USA. (meade@fas.harvard.edu)